PAPER

Check for updates

Reactivity of copper(I) complexes supported by tripodal nitrogen-containing tetradentate ligands toward gaseous diatomic molecules, NO, CO and O_2†

Yuma Morimoto, [iD] *‡ Keisuke Inoue and Shinobu Itoh [iD] *

Series of Cu(I) complexes supported by nitrogen-based tetradentate ligands were examined for their reactivity toward nitric oxide (NO). The copper complexes generated the corresponding Cu(II)−nitrite complexes in the presence of an excess molar amount of NO. A higher reactivity of the Cu(I) complexes toward NO was observed with a more negative Cu(I/II) redox potential, same as their reactivity toward O_2 and CO, while $[Cu^I(tepa)]^+$ with the most positive oxidation potential only reacted with NO among the diatomic gaseous molecules (NO, O_2, and CO) examined in this study. DFT studies explained that the reactivity of the Cu−NO complex was the key to its selectivity rather than its coordination bond stability.

Introduction

Nitric oxide (NO) plays significant roles in many bio-physiological processes.[1] Bacteria generate NO from nitrite ions (NO_2^-) and further reduce this to nitrous oxide (N_2O) in the course of their anaerobic respiration, which is part of the geochemical nitrogen cycle.[2] In mammals, NO is synthesized *via* the oxidation of L-arginine as a secondary messenger, neurotransmitter, or cytotoxic agent.[3,4] In these NO-related processes, metalloenzymes containing iron, copper, or molybdenum play essential roles.[5] Copper-containing nitrite reductase (CuNiR) plays a pivotal role in the conversion of NO_2^- to NO and the reverse reaction.[6–10] Furthermore, CuNiR has been reported to catalyse NO reduction to N_2O.[11] Such divergent reactivity of the same enzyme is derived from the redox flexibility of NO, which can act as either an electron donor or electron acceptor in metal/NO interactions. Thus, it would be of great interest to clarify the mechanistic details of these processes occurring at the copper centre of the enzyme. On a related note, copper-ion-loaded zeolites have been reported to effectively decompose NO_x, suggesting that the

reaction involving N_2O formation from NO likely shares a common mechanism.[12]

To understand details of the NO chemistry in enzymatic systems, several model studies of CuNiR have been conducted over the last few decades. For instance, Tolman and co-workers reported the reaction between NO and Cu(I) complexes supported by a Tp (Tp: hydrotris(pyrazolyl)borate) ligand to form N_2O and NO_2^-, which is also seen in CuNiR.[13] They also succeeded in isolating an intermediate species of the reaction, *i.e.*, the Cu−NO adduct. Cu(I) complexes of tmpa (tris(pyridin-2-ylmethyl)amine) and tacn (1,4,7-triazacyclononane) were also found to show reactivity toward NO. However, there has been little exploration to date regarding the factors that control NO reactivity.[14]

In this study, we systematically investigated the reactivity of Cu(I) complexes supported by a series of tripodal nitrogen-containing tetradentate ligands (Fig. 1) towards NO. All these carefully designed neutral tripodal ligands feature a central alkylamine nitrogen and three sp^2 nitrogen donor groups, providing a well-defined platform to elucidate structure–reactivity relationships. To gain comprehensive insights into the NO chemistry of these copper complexes, we also examined their reactivity towards O_2 and CO, allowing for a comparative analysis.

Department of Applied Chemistry, Graduate School of Engineering, Osaka University, 2-1 Yamada-oka, Suita, Osaka 565-0871, Japan.
E-mail: yuma.morimoto@chem.sci.isct.ac.jp, shinobu@mls.eng.osaka-u.ac.jp
†Electronic supplementary information (ESI) available. CCDC 2392146, 2392088 and 2391963. For ESI and crystallographic data in CIF or other electronic format see DOI: https://doi.org/10.1039/d4dt03001j
‡Current Address: Department of Chemistry, School of Science, Institute of Science Tokyo, 2-12-1 Ookayama, Meguro-ku, Tokyo 152-8550, Japan.

Results and discussion

Reactivity of Cu(I) complexes toward NO

Cu(I) complexes supported by tripodal nitrogen-containing tetradentate ligands, namely, $[Cu^I(tepa)](OTf)$,[15] $[Cu^I(tmqa)]$ (OTf),[16] $[Cu^I(tmpa)(CH_3CN)](OTf)$,[17] and $[Cu^I(TMG_3tren)]$
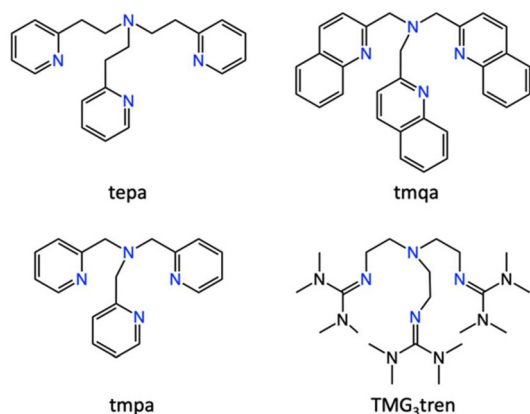
Fig. 1 Structures of the supporting ligands employed in this work. tepa: tris(2-(pyridin-2-yl)ethyl)amine, tmqa: tris(quinolin-2-ylmethyl)amine, tmpa: tris(pyridine-2-ylmethyl)amine, and TMG₃tren: tris(2-(N-tetramethylguanidyl)ethyl)-amine.

(OTf),[18] were prepared according to the reported procedures. Reactions of the Cu(I) complexes and NO were followed by UV-vis spectroscopy (Fig. 2). Upon an addition of excess NO(g) into a THF solution of $[Cu^I(tepa)]^+$, the MLCT band of the Cu(I) complex (340 nm, $\varepsilon = 9800\ M^{-1}\ cm^{-1}$) decreased, and the d-d band at 620 nm ($\varepsilon = 170\ M^{-1}\ cm^{-1}$) concomitantly increased, also showing a clean isosbestic point at 410 nm (Fig. 2a). However, decay of the Cu(I) absorption band remained incomplete due to the reactivity of the generated Cu(II) complex toward NO.§ Even in the presence of an excess molar amount of NO to Cu(I), the time course did not obey first-order kinetics. The generated absorption band at 620 nm was identical to that of $[Cu^{II}(tepa)(ONO)]^+$, which was synthesized separately, and the yield was determined to be 40% based on a comparison of the absorption intensity. The formation of $[Cu^{II}(tepa)(ONO)]^+$ was also confirmed by X-ray crystallography of a single crystal obtained from the resulting solution. Fig. 3a shows the crystal structure of $[Cu^{II}(tepa)(ONO)]^+$, while its crystallographic data are summarized in Table S1 in the ESI.† It was found that the nitrite ion (NO_2^-) was coordinated to the copper centre with a κ^2-O,O binding mode having weak interaction with the distal oxygen atoms (Cu1–O1, 2.027(2) Å; Cu1–O2, 2.644(2) Å). Thus, the copper centre exhibited a square pyramidal geometry ($\tau_5 = 0.05$), where the basal plane consisted of two pyridine nitrogen atoms (N2 and N4), the alkylamine nitrogen (N1) and the oxygen atom of NO_2^- (O1), with the axial position occupied by the remaining pyridine atom (N3).[19]

Reactivities of $[Cu^I(tmqa)]^+$ and $[Cu^I(TMG_3tren)]^+$ toward NO were also examined in THF at 25 °C. Upon the addition of NO gas into the solution of each Cu(I) complex, there was a decrease in the MLCT band ($\lambda_{max} = 375$ nm, $\varepsilon = 9400\ M^{-1}\ cm^{-1}$ and around 370 nm) and an increase in the d–d band ($\lambda_{max} = 680$ nm, $\varepsilon = 120\ M^{-1}\ cm^{-1}$ and $\lambda_{max} = 720$ nm and 1000 nm,
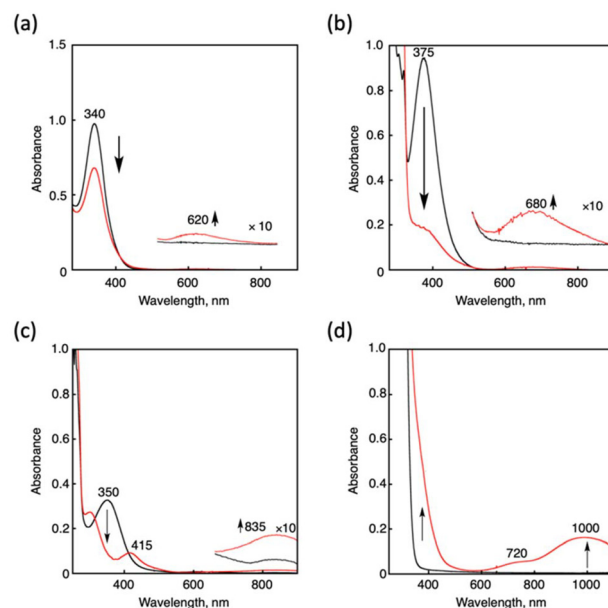

Fig. 2 UV-vis spectral changes observed after NO gas bubbling into deaerated THF solution containing the Cu(I) complexes ($[Cu^I(tepa)](OTf)$ (0.10 mM) (a), $[Cu^I(tmqa)](OTf)$ (0.10 mM) (b), $[Cu^I(tmpa)(CH_3CN)](OTf)$ (0.10 mM) (c), and $[Cu^I(TMG_3tren)](OTf)$ (0.50 mM) (d)) at 25 °C. Black and red lines show the initial and resulting spectra, respectively, measured after 5000 s (a), 40 000 s (b), 10 s (c), and 300 s (d).

$\varepsilon_{1000} = 320\ M^{-1}\ cm^{-1}$), as shown in Fig. 2b and d.¶ The products were determined as Cu(II) nitrite complexes, namely, $[Cu^{II}(tmqa)(ONO)]^+$ and $[Cu^{II}(TMG_3tren)(ONO)]^+$, respectively, by comparison of the solution spectra of the authentic samples and X-ray analysis of the crystals obtained from the resulting solution as per the tepa system described above (Fig. 3b and c).‖ $[Cu^{II}(tmqa)(ONO)]^+$ and $[Cu^{II}(TMG_3tren)(ONO)]^+$ also included a nitrite ion coordinated to the Cu centre in κ^2-O,O and κ^1-O binding modes, respectively. The distal oxygen atom of NO_2^- interacts with the Cu centre in $[Cu^{II}(tmqa)(ONO)]^+$ as well as $[Cu^{II}(tepa)(ONO)]^+$, whereas that of $[Cu^{II}(TMG_3tren)(ONO)]^+$ was located outside of the copper coordination sphere because of the bulkiness of the TMG group. It was found that $[Cu^{II}(tmqa)(ONO)]^+$ has a square pyramidal structure ($\tau_5 = 0.03$), whereas $[Cu^{II}(TMG_3tren)(ONO)]^+$ has a slightly distorted trigonal bipyramidal structure with $\tau_5 = 0.83$, which is a typical geometry of tren ligands. Karlin and co-workers reported that the reaction of $[Cu^I(tmpa)]^+$ and NO in THF gave $[(tmpa)Cu^{II}-ONO]^{2+}$.[20] We also confirmed the formation of $[Cu^{II}(tmpa)(ONO)]^+$ in THF with absorption maxima at 300, 415 and 835 nm (Fig. 2c). The reaction of $[Cu^I(tepa)]^+$ and $[Cu^I(tmqa)]^+$ with NO took more than 10 000 s, whereas $[Cu^I(tmpa)(CH_3CN)]^+$ and $[Cu^I(TMG_3tren)]^+$ were readily con-

---

§ $[Cu^{II}(tepa)]^{2+}$ separately prepared was found to react with NO to form $[Cu^I(tepa)]^+$. Details of the reaction will be described elsewhere.

¶ The time courses of reactions did not follow the first-order kinetics, preventing quantitative determination of the reaction rate constants.

‖ ESI-MS analyses of the LCu(II)–nitrite complexes were hampered by the instability of the complex under mass spectrometry conditions, resulting in peaks corresponding only to LCu(II) complexes.
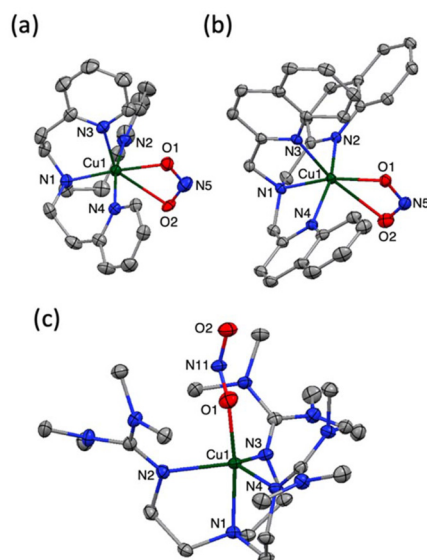
Fig. 3 ORTEP drawings of (a) [Cu^{II}(tepa)(ONO)](OTf), (b) [Cu^{II}(tmqa)(ONO)] (OTf), and (c) [Cu^{II}(TMG$_3$tren)(ONO)](OTf) showing 50% probability thermal ellipsoids. The counter anion, solvent molecule, and hydrogen atoms are omitted for clarity.
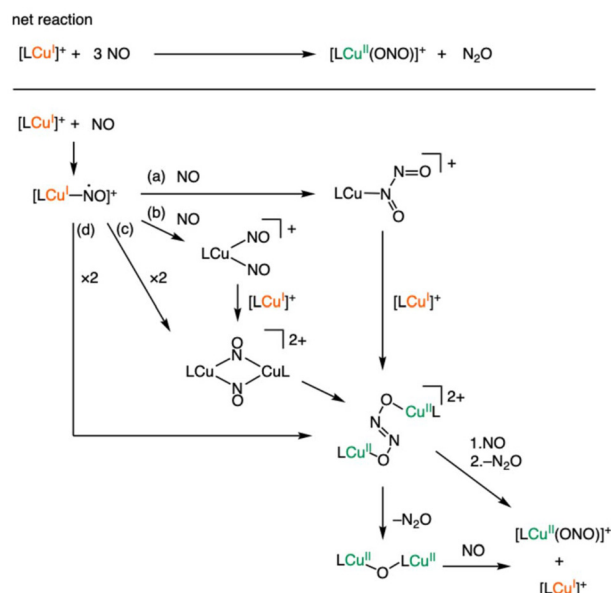

Scheme 1 Possible reaction pathways between the Cu(I) complexes and NO.

verted into the Cu(II) complexes (*vide infra*). GC-MS analysis of the generated gas product revealed the formation of N$_2$O gas in the reaction of [Cu^{I}(TMG$_3$tren)]$^+$, whereas the [Cu^{I}(tepa)]$^+$ and [Cu^{I}(tmqa)]$^+$ system did not generate N$_2$O, which was possibly due to the inefficiency of the reaction.

The reaction between Cu(I) complexes and NO has been reported to form N$_2$O and NO$_2^-$, though the exact mechanism remains elusive.[14a,21] Karlin's group identified the formation of [(tmpa)$_2$Cu$_2^{II}$(μ-N$_2$O$_2^{2-}$)]$^{2+}$, supported by crystallographic evidence.

The formation of the Cu$_2^{II}$(μ-N$_2$O$_2^{2-}$) complex is outlined as a stepwise process involving (i) Cu–NO bond formation, (ii) dinuclear complex formation and (iii) N–N bond formation. Several potential intermediates were incorporated in Scheme 1, including [LCu(N$_2$O$_2$)]$^+$, [LCu(NO)$_2$]$^+$ and [LCu$_2$(μ-NO)$_2$]$^{2+}$, proposed by Tolman's group.[14a,21] Our experimental investigation of [Cu^{I}(TMG$_3$tren)]$^+$ suggests that pathways (b) and (c), involving the coordination of two NO molecules on a copper centre are unlikely to occur. This conclusion arises from the steric constraints imposed by the three tetramethyl-guanidino groups, which may hinder the simultaneous binding of two NO molecules within the confined coordination environment. In the later calculational study section, we discuss the formation process and conversion process of the Cu$_2^{II}$(μ-N$_2$O$_2^{2-}$) complex to form Cu^{II}(ONO$^-$) based on the chemical stability of each intermediate.

Reactivity of Cu(I) complexes toward O$_2$ and CO

Cu(I) complexes exhibit distinct reactivity toward O$_2$ and CO due to their different coordination modes. Typically, O$_2$ binds to the copper center as an X-type ligand, whereas CO acts as an L-type ligand, characterized by strong π-back donation. We

analyzed the reactivity of Cu(I) complexes toward O$_2$ and CO from the perspective of the oxidation potential, incorporating previously reported findings as outlined below. As shown in Fig. 4, [Cu^{I}(tepa)]$^+$ reacted with neither O$_2$ nor CO, as also
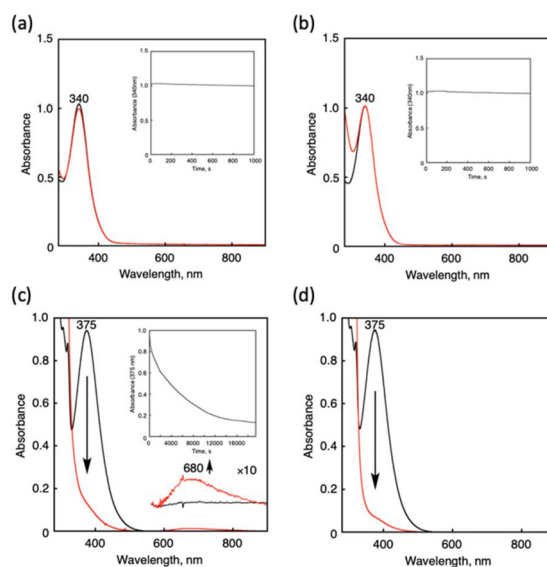

Fig. 4 UV-vis spectral changes of [Cu^{I}(tepa)]$^+$ (0.1 mM) in the presence of excess (a) O$_2$ and (b) CO gas in THF at 25 °C. Black line: initial spectra of the Cu(I) complexes; red line: spectra obtained after the addition of O$_2$ (1000 s) or CO gas (1000 s). Inset: time course of the UV-vis spectral changes followed at 340 nm. UV-vis spectral changes of [Cu^{I}(tmqa)]$^+$ (0.10 mM) in the presence of excess (c) O$_2$ and (d) CO gas in THF at 25 °C. Black line: initial spectra of the Cu(I) complexes; red line: spectra obtained after the addition of O$_2$ (200 000 s) or CO gas (10 s). Inset: time course of the UV-vis spectral changes followed at 375 nm.

Table 1 Correlation between the reactivity and redox potentials of Cu(I) complexes

Complex	$E_{1/2}$ [a]	Reactivity [b]		
		NO	O_2	CO
$[Cu^I(TMG_3tren)]^+$	−0.28	Fast[c]	Fast[c]	Fast[c]
$[Cu^I(tmpa)(CH_3CN)]^+$	−0.02	Fast[c]	Fast[c]	Fast[c]
$[Cu^I(tmqa)]^+$	0.35	2×10^4	4×10^4	Fast[c]
$[Cu^I(tepa)]^+$	0.44	3×10^3	N.R.[d]	N.R.[d]

[a] Versus SCE. [b] Evaluated by the half-life time of the reaction. [c] Half-life time is less than 50 s. [d] Not reacted.

reported by Karlin and co-workers (Fig. 4a and b).[15,22]** Notably, $[Cu^I(tepa)]^+$ only reacted with NO without showing any reactivity toward O_2 and CO. Such a copper complex has never been reported so far. $[Cu^I(tmqa)]^+$ showed sluggish reactivity toward O_2 in THF at 25 °C and was oxidized to a Cu(II) complex slowly under an O_2 atmosphere in two days (Fig. 4c).[16] Conversely, $[Cu^I(tmqa)]^+$ immediately reacted with CO to generate a Cu-CO adduct (Fig. 4d). In the case of tmpa and TMG_3tren systems, the Cu(I) complexes showed high reactivity toward O_2 and CO under identical experimental conditions to those used for the tepa and tmqa systems (Table 1). As reported, $[Cu^I(tmpa)(CH_3CN)]^+$ and $[Cu^I(TMG_3tren)]^+$ reacted with O_2 even at a low temperature (−80 °C) to provide a dinuclear Cu(II) end-on peroxide complex[17,23] and a mononuclear Cu(II) end-on superoxide complex,[24] respectively. These complexes also showed high reactivities toward CO to provide Cu-CO adducts.[17,25] From the results, it became clear that these Cu(I) complexes showed different reactivities toward gaseous molecules though they had similar tetradentate-tripod ligands. The difference in reactivity may have resulted from their difference in electronic structures (*vide infra*).

Electrochemical property

Oxidation potentials of the Cu(I) complexes were determined by cyclic voltammetry (CV) to get insights into the differences in their reactivities (Fig. 5). The cyclic voltammograms of $[Cu^I(TMG_3tren)]^+$, $[Cu^I(tmpa)(CH_3CN)]^+$, $[Cu^I(tmqa)]^+$, and $[Cu^I(tepa)]^+$ exhibited reversible Cu(I)/Cu(II) redox couples at $E_{1/2}$ = −0.28 V, −0.02 V, 0.35 V and 0.44 V *vs.* SCE in CH_3CN, respectively. The oxidation potentials of $[Cu^I(tmpa)(CH_3CN)]^+$ and $[Cu^I(tepa)]^+$ showed a significant gap of 0.46 V, regardless of their same ligand-donor sets. The more positive oxidation potential of $[Cu^I(tepa)]^+$ was ascribed to its tetrahedral geometry (τ_4 = 0.840), which could stabilize the Cu(I) state, also having an impact on the MLCT energy and its coefficient (Fig. 2a and c). As the redox potentials of the copper complexes became negative, the reactivities of the Cu(I) complexes toward the diatomic molecules became higher (Table 1). It is well known that the reactions between transition-metal complexes

**A small increase in absorption around 300 nm can be ascribed to the formation of the CO complex, although we cannot detect any other spectroscopic evidence using ^1H NMR and IR measurement.
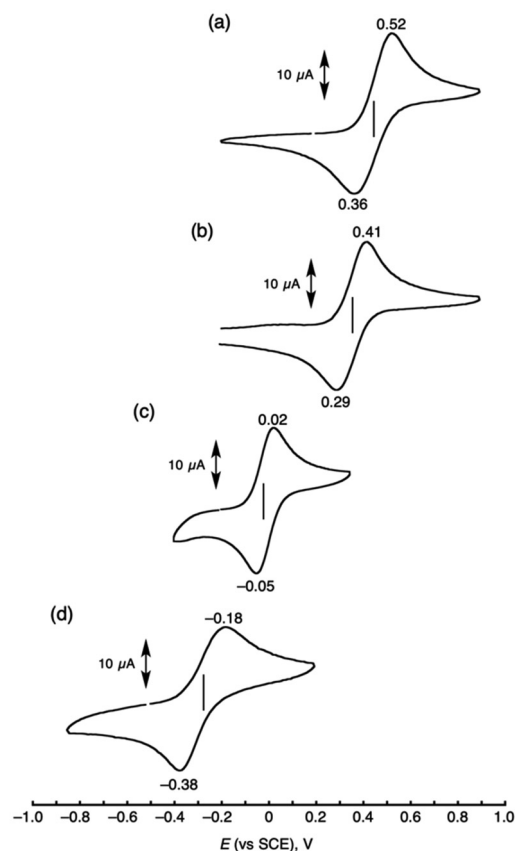

Fig. 5 Cyclic voltammograms of $[Cu^I(tepa)]^+$ (a), $[Cu^I(tmqa)]^+$ (b), $[Cu^I(tmpa)(CH_3CN)]^+$ (c), and $[Cu^I(TMG_3tren)]^+$ (d) (1.0 mM) in dry acetonitrile containing $TBAPF_6$ (0.10 M) under a N_2 atmosphere; working electrode: glassy carbon, counter electrode: Pt, and reference electrode: $Ag/AgNO_3$ (10 mM). Scan rate was 100 mV s^{-1}.

and O_2 or CO are mainly governed by the electron-donation ability of the metal to O_2 or CO.[26] The similar tendency in reactivity toward NO suggests that the reactivity of the Cu(I) complexes with NO also depended on the electron-donation ability of the Cu(I) complexes when tripodal tetradentate ligands are employed. Judging from the very negative one-electron reduction potential of NO (−1.05 V *vs.* SCE),[27,28] the reaction between the Cu(I) complex and NO could not be an outer sphere electron-transfer reaction but requires significant orbital overlaps.

DFT calculations

To elucidate the reaction selectivity of $[Cu^I(tepa)]^+$ complex toward NO over CO and O_2, the electronic structures of $[Cu(tepa)(NO)]^+$, $[Cu(tepa)(CO)]^+$ and $[Cu(tepa)(O_2)]^+$ were investigated using DFT calculations at the UB3LYP-D3BJ functional level with the def2-SVP basis set. Optimized structures of the NO and O_2 adducts of the Cu(I)-tepa complex were obtained as penta-coordinate complexes with distorted square pyramidal geometries. The diatomic molecules coordinated to the trans-position of the *tert*-alkyl amine nitrogen had the highest donor ability. Alternatively, the CO complex took a tetrahedral geome-

try, where one of the pyridine nitrogens was detached from the copper center (Cu–N = 3.04 Å) but still had an interaction *via* a π-coordination mode. The Gibbs free energy changes by the coordination of $[Cu^I(tepa)]^+$ with NO, CO and O_2 were evaluated to be endothermic, with values of 7.75, 4.86 and 4.84 kcal mol^{-1}, respectively. In all the cases, the electronic energies were stabilized by the coordination of the gaseous molecules, while the entropy term made the coordination endothermic. In contrast to the experimental results, NO binding to $[Cu^I(tepa)]^+$ was the most unfavourable process. Therefore, the reaction selectivity of $[Cu^I(tepa)]^+$ toward NO can be explained by the reaction heat of the subsequent reaction of $[Cu^I(tepa)(NO)]^+$ with another NO molecule, as shown in Scheme 1.

As mentioned above, CO and O_2 interact with Cu(I) complexes in different ways, although both ligands prefer more electron-rich Cu(I) centres. The Cu(I)–CO complex is primarily stabilized through π-back donation. By contrast, in the end-on copper–O_2 complex, the main interaction involved σ-donation from the superoxide ($O_2^{\bullet-}$) to the Cu(II) centre produced by electron transfer from Cu(I) to O_2. The NO ligand, which has an intermediate number of electrons and orbital energy, has the potential to interact with Cu(I) complex *via* both mechanisms. Electrons in the π* orbitals of NO and O_2 occupy anti-bonding character orbitals between the copper centre and the ligand, weakening the coordination bond (Fig. S1a–c†). This weakening is reflected in the Wiberg bond index (WBI);[29] whereby the Cu–CO, Cu–NO, and Cu–O_2 complexes had bond orders of 0.83, 0.41 and 0.20, respectively. Despite the decrease in WBI for the Cu–CO, Cu–NO and Cu–O_2 complexes, the lowest unoccupied Kohn–Sham orbital energy levels of the diatomic molecules (−0.81, −2.84 and −3.02 eV, respectively) approached the HOMO energy level of $[Cu^I(tepa)]^+$ (−7.99 eV), facilitating the formation of more stable coordination bonds. A comparison of the NPA (natural population analysis) charges suggests that electrostatic interaction between the copper center and the ligand are also critical in determining the stability of the complexes. Among the systems, the Cu–O_2 complex had the most positively charged copper center (NPA charge: 0.74) and the most negatively charged coordinating atom (NPA charge on O_2: −0.09). The valence of two factors, namely, π-back donation and σ-donation, resulted in the Cu–NO complex being the most unstable among the three complexes. In the Cu–NO complex, the NO ligand moiety accepted the largest amount of electron density among the three systems (NPA charge on NO: −0.41). Structural parameters (∠Cu–N–O = 118.5°, d_{N-O} = 1.17 Å, $\tilde{\nu}_{N-O}$ = 1814 cm^{-1}) were assignable to the NO in a reduced state. The electron transfer from the Cu(I) centre to the NO ligand may control the reaction process, as suggested by the clear correlation observed between the oxidation potential of the Cu(I) complexes and their reactivities toward NO (Fig. 6).

We also performed computational evaluations on the plausible reaction pathway shown in Scheme 1. Herein, the dinitrogen dioxide complex [LCu–N(O)–NO], formed by the second addition of NO to the Cu–NO complex, was calculated to be more unstable than the Cu–NO complex (8.00 kcal mol^{-1}, Fig. 7). The Cu–N and N–N bond lengths were found to be 2.86 and 1.93 Å, respectively,
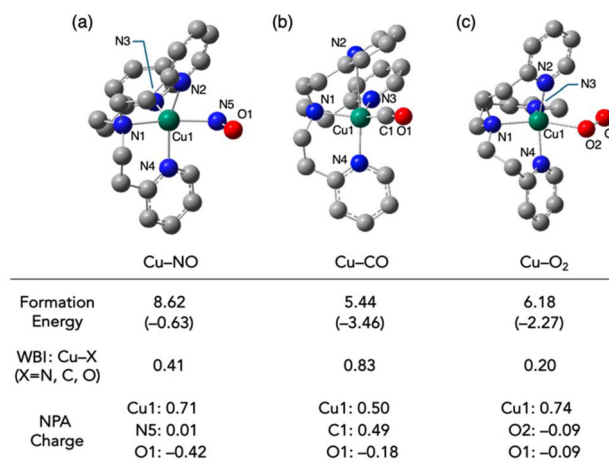

Fig. 6 Optimized structures of (a) $[Cu(tepa)(NO)]^+$, (b) $[Cu(tepa)(CO)]^+$ and (c) $[Cu(tepa)(O_2)]^+$ calculated by DFT at the B3LYP-D3BJ/def2-SVP level. Formation energies [electronic energy (shown in parenthesis) with the thermal energy correction] from their precursors, namely, $[Cu(tepa)]^+$ and diatomic molecule, Wiberg bond index values between the copper center and the coordinating atom, and NPA charges of the selected atoms are shown together.

	Cu–NO	Cu–CO	Cu–O_2
Formation Energy	8.62 (−0.63)	5.44 (−3.46)	6.18 (−2.27)
WBI: Cu–X (X=N, C, O)	0.41	0.83	0.20
NPA Charge	Cu1: 0.71 N5: 0.01 O1: −0.42	Cu1: 0.50 C1: 0.49 O1: −0.18	Cu1: 0.74 O2: −0.09 O1: −0.09

indicating the absence of strong interactions between the copper centre and the nitrogen atoms. The distal nitrogen atom was positioned at a distance of 3.01 Å from the copper centre, indicating that the optimized structure was indistinguishable from a Cu-dinitrosyl complex $[LCu-(NO)_2]$. The second addition of nitrosyl ligand was thus thermodynamically unfavourable. The dimerization of the [LCu–(NO)] complex to form di(μ-nitroso-k^1N)dicopper $[LCu(NO)_2CuL]$ was also estimated to be an energetically unfavourable process with 24.93 kcal mol^{-1}. By contrast, μ-hyponitritodicopper [LCu(ONNO)CuL] was estimated to be a thermodynamically favourable intermediate with a stabilization energy of −10.30 kcal mol^{-1} relative to LCu–NO. This intermedi-
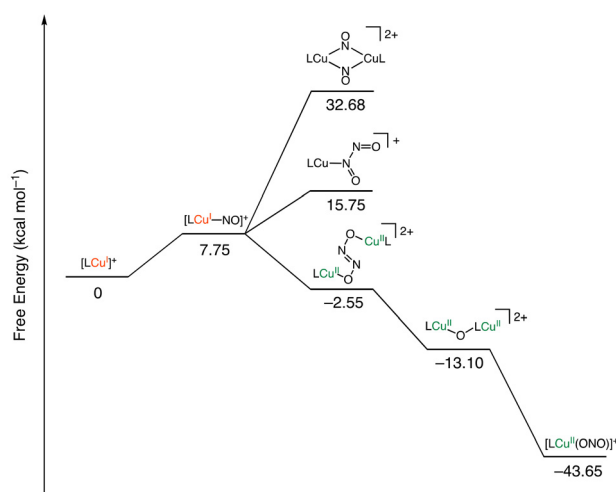

Fig. 7 Calculated free energies for the plausible intermediates in the reaction of $[LCu^I]^+$ (L = tepa) with NO to form $[LCu^{II}(NO_2)]^+$ and N_2O.

ate was −2.55 kcal mol⁻¹ lower in energy and thus more stable than the starting materials. The dissociation of nitrous oxide from [LCu(ONNO)CuL] to yield the μ-oxidodicopper complex (LCu–O–CuL) was calculated to be an exothermic process (−10.55 kcal mol⁻¹). Furthermore, the final nitritocopper(ɪɪ) complex was more stable than LCu–O–CuL by −30.55 kcal mol⁻¹. Our computational results suggest that Path d in Scheme 1 is the most reasonable. Given the sufficient reaction exothermicity to release N₂O, the stepwise mechanism *via* the μ-oxidodicopper complex appears to be the most plausible pathway.

Conclusion

A series of Cu(ɪ) complexes supported by tripodal tetradentate ligands was employed to investigate the controlling factors in the reaction between the Cu(ɪ) complexes and NO. The reactivity of the complexes were also examined toward CO and O₂ to understand the characteristics of NO. All the Cu(ɪ) complexes reacted with NO, and the formation of Cu(ɪɪ)–nitrite complexes were confirmed in the tepa, tmqa and TMG₃tren systems. The Cu(ɪ) complexes also showed reactivity toward O₂ and CO, except for [Cuᴵ(tepa)]⁺. Generally, Cu(ɪ) complexes of TMG₃tren and tmpa showed higher reactivity toward diatomic molecules than the Cu(ɪ) complexes supported by tmqa and tepa ligands. Such a tendency was consistent with the order of the oxidation potentials of the Cu(ɪ) complexes. Among the Cu(ɪ) complexes examined in this study, [Cuᴵ(tepa)]⁺, having a very positive $E_{1/2}$ value, was found to exhibit unique reaction selectivity toward NO over O₂ and CO. Based on the DFT study, the NO molecule binding to the copper centre was estimated to be weaker than the binding of CO and O₂; however, in the following reaction, to form thermodynamically favourable product, N₂O and NO₂⁻ facilitated the conversion of Cu(ɪ) complex to the corresponding Cu(ɪɪ) complex. This explanation is consistent with the slower reaction of NO with [Cuᴵ(tmqa)]⁺ than that of CO and O₂. This is the first report to demonstrate that the oxidation potential of Cu(ɪ) complexes controls their reactivity toward NO when the copper complexes have a similar coordination geometry. This finding provides a valuable insight into understanding the role of copper-containing NO reductase and the NO conversion reaction involving Cu(ɪ) ions existing in biological systems.

Author contributions

YM led the conceptualization, funding acquisition, quantum calculation and review & editing of the work, KI conducted data curation and wrote the original draft and SI supervised the work and finalized the manuscript.

Data availability

The data supporting this article have been included as part of the ESI.† CCDC 2391963, 2392088 and 2392146† contain crys-

tallographic data for [Cuᴵᴵ(tepa)(ONO)](OTf), [Cuᴵᴵ(tmqa)(ONO)](OTf), and [Cuᴵᴵ(TMG₃tren)(ONO)](OTf), respectively.

Conflicts of interest

There are no conflicts to declare.

Acknowledgements

References

1 (*a*) A. R. Butler and D. L. H. Williams, The physiological role of nitric oxide, *Chem. Soc. Rev.*, 1993, **22**(4), 233–241; (*b*) L. J. Ignarro and B. Freeman, *Nitric Oxide: Biology and Pathobiology*, Elsevier Science, 2017.

2 (*a*) L. I. Hochstein and G. A. Tomlinson, The Enzymes Associated with Denitrification, *Annu. Rev. Microbiol.*, 1988, **42**, 231–261; (*b*) B. A. Averill, Dissimilatory Nitrite and Nitric Oxide Reductases, *Chem. Rev.*, 1996, **96**(7), 2951–2964; (*c*) W. J. Payne, *Denitrification*, Wiley, 1981.

3 R. M. Palmer, D. D. Rees, D. S. Ashton and S. Moncada, L-arginine is the physiological precursor for the formation of nitric oxide in endothelium-dependent relaxation, *Biochem. Biophys. Res. Commun.*, 1988, **153**(3), 1251–1256.

4 M. W. Radomski, R. M. J. Palmer and S. Moncada, Characterization of the L-arginine: nitric oxide pathway in human platelets, *Br. J. Pharmacol.*, 1990, **101**(2), 325–328.

5 A. Sigel, H. Sigel and R. K. O. Sigel, *Biogeochemical cycles of elements; Metal ions in biological systems*, Taylor & Francis, 2005, vol. 43.

6 J. W. Godden, S. Turley, D. C. Teller, E. T. Adman, M. Y. Liu, W. J. Payne and J. LeGall, The 2.3 Angstrom X-Ray Structure of Nitrite Reductase from *Achromobacter cycloclastes*, *Science*, 1991, **253**(5018), 438–442.

7 S. Suzuki, K. Kataoka and K. Yamaguchi, Metal Coordination and Mechanism of Multicopper Nitrite Reductase, *Acc. Chem. Res.*, 2000, **33**(10), 728–735.

8 M. E. P. Murphy, S. Turley and E. T. Adman, Structure of Nitrite Bound to Copper-containing Nitrite Reductase from *Alcaligenes faecalis*: Mechanistic Implications, *J. Biol. Chem.*, 1997, **272**(45), 28455–28460.

9 E. I. Tocheva, F. I. Rosell, A. G. Mauk and M. E. P. Murphy, Side-On Copper-Nitrosyl Coordination by Nitrite Reductase, *Science*, 2004, **304**(5672), 867–870.

10 E. I. Solomon, D. E. Heppner, E. M. Johnston, J. W. Ginsbach, J. Cirera, M. Qayyum, M. T. Kieber-Emmons, C. H. Kjaergaard, R. G. Hadt and L. Tian, Copper Active Sites in Biology, *Chem. Rev.*, 2014, **114**(7), 3659–3853.

11 (*a*) C. L. Hulse, J. M. Tiedje and B. A. Averill, Evidence for a copper-nitrosyl intermediate in denitrification by the copper-containing nitrite reductase of Achromobacter cycloclastes, *J. Am. Chem. Soc.*, 1989, **111**(6), 2322–2323; (*b*) S. Ghosh, A. Dey, O. M. Usov, Y. Sun, V. M. Grigoryants, C. P. Scholes and E. I. Solomon, Resolution of the Spectroscopy versus Crystallography Issue for NO Intermediates of Nitrite Reductase from Rhodobacter sphaeroides, *J. Am. Chem. Soc.*, 2007, **129**(34), 10310–10311.

12 (*a*) F. Gao, D. Mei, Y. Wang, J. Szanyi and C. H. F. Peden, Selective Catalytic Reduction over Cu/SSZ-13: Linking Homo- and Heterogeneous Catalysis, *J. Am. Chem. Soc.*, 2017, **139**(13), 4935–4942; (*b*) P. Granger and V. I. Parvulescu, Catalytic NOx Abatement Systems for Mobile Sources: From Three-Way to Lean Burn after-Treatment Technologies, *Chem. Rev.*, 2011, **111**(5), 3155–3207; (*c*) J. H. Kwak, D. Tran, J. Szanyi, C. H. F. Peden and J. H. Lee, The Effect of Copper Loading on the Selective Catalytic Reduction of Nitric Oxide by Ammonia Over Cu-SSZ-13, *Catal. Lett.*, 2012, **142**(3), 295–301.

13 S. M. Carrier, C. E. Ruggiero, W. B. Tolman and G. B. Jameson, Synthesis and structural characterization of a mononuclear copper nitrosyl complex, *J. Am. Chem. Soc.*, 1992, **114**(11), 4407–4408.

14 (*a*) P. P. Paul and K. D. Karlin, Functional modeling of copper nitrite reductases: reactions of NO_2^- or nitric oxide with copper(I) complexes, *J. Am. Chem. Soc.*, 1991, **113**(16), 6331–6332; (*b*) S. Mahapatra, J. A. Halfen and W. B. Tolman, Catalytic reduction of nitric oxide to nitrous oxide by alcohols mediated by copper(I) complexes, *J. Chem. Soc., Chem. Commun.*, 1994, (14), 1625–1626.

15 K. D. Karlin, J. C. Hayes, J. P. Hutchinson, J. R. Hyde and J. Zubieta, Synthesis and X-ray structural characterization of Cu(I) and Cu(II) derivatives of a new symmetric tripodal ligand $N(CH_2CH_2\text{-}py)_3$, (py = 2-pyridyl), *Inorg. Chim. Acta*, 1982, **64**, L219–L220.

16 N. Wei, N. N. Murthy, Q. Chen, J. Zubieta and K. D. Karlin, Copper(I)/Dioxygen Reactivity of Mononuclear Complexes with Pyridyl and Quinolyl Tripodal Tetradentate Ligands: Reversible Formation of Cu : O_2 = 1 : 1 and 2 : 1 Adducts, *Inorg. Chem.*, 1994, **33**(9), 1953–1965.

17 R. R. Jacobson, Z. Tyeklar, A. Farooq, K. D. Karlin, S. Liu and J. Zubieta, A copper-oxygen (Cu_2–O_2) complex. Crystal structure and characterization of a reversible dioxygen binding system, *J. Am. Chem. Soc.*, 1988, **110**(11), 3690–3692.

18 V. Raab, J. Kipke, O. Burghaus and J. Sundermeyer, Copper Complexes of Novel Superbasic Peralkylguanidine

Derivatives of Tris(2-aminoethyl)amine as Constraint Geometry Ligands, *Inorg. Chem.*, 2001, **40**(27), 6964–6971.

19 L. Yang, D. R. Powell and R. P. Houser, Structural Variation in Copper(I) Complexes with Pyridylmethylamide Ligands: Structural Analysis with a New Four-coordinate Geometry Index, τ_4, *Dalton Trans.*, 2007, (9), 955–964.

20 G. B. Wijeratne, S. Hematian, M. A. Siegler and K. D. Karlin, Copper(I)/NO(g) Reductive Coupling Producing a trans-Hyponitrite Bridged Dicopper(II) Complex: Redox Reversal Giving Copper(I)/NO(g) Disproportionation, *J. Am. Chem. Soc.*, 2017, **139**(38), 13276–13279.

21 C. E. Ruggiero, S. M. Carrier and W. B. Tolman, Reductive Disproportionation of NO Mediated by Copper Complexes: Modeling N_2O Generation by Copper Proteins and Heterogeneous Catalysts, *Angew. Chem., Int. Ed. Engl.*, 1994, **33**(8), 895–897.

22 S. Itoh and Y. Tachi, Structure and O_2-reactivity of copper(I) complexes supported by pyridylalkylamine ligands, *Dalton Trans.*, 2006, (38), 4531–4538.

23 Z. Tyeklar, R. R. Jacobson, N. Wei, N. N. Murthy, J. Zubieta and K. D. Karlin, Reversible reaction of dioxygen (and carbon monoxide) with a copper(I) complex. X-ray structures of relevant mononuclear Cu(I) precursor adducts and the trans-(.mu.-1,2-peroxo)dicopper(II) product, *J. Am. Chem. Soc.*, 1993, **115**(7), 2677–2689.

24 C. Würtele, E. Gaoutchenova, K. Harms, M. C. Holthausen, J. Sundermeyer and S. Schindler, Crystallographic Characterization of a Synthetic 1 : 1 End-on Copper Dioxygen Adduct Complex, *Angew. Chem., Int. Ed.*, 2006, **45**(23), 3867–3869.

25 H. C. Fry, H. R. Lucas, A. A. Narducci Sarjeant, K. D. Karlin and G. J. Meyer, Carbon Monoxide Coordination and Reversible Photodissociation in Copper(I) Pyridylalkylamine Compounds, *Inorg. Chem.*, 2008, **47**(1), 241–256.

26 (*a*) L. M. Mirica, X. Ottenwaelder and T. D. P. Stack, Structure and Spectroscopy of Copper−Dioxygen Complexes, *Chem. Rev.*, 2004, **104**(2), 1013–1046; (*b*) E. A. Lewis and W. B. Tolman, Reactivity of Dioxygen−Copper Systems, *Chem. Rev.*, 2004, **104**(2), 1047–1076.

27 M. D. Bartberger, W. Liu, E. Ford, K. M. Miranda, C. Switzer, J. M. Fukuto, P. J. Farmer, D. A. Wink and K. N. Houk, The reduction potential of nitric oxide (NO) and its importance to NO biochemistry, *Proc. Natl. Acad. Sci. U. S. A.*, 2002, **99**(17), 10958–10963.

28 A. S. Dutton, J. M. Fukuto and K. N. Houk, Theoretical Reduction Potentials for Nitrogen Oxides from CBS-QB3 Energetics and (C)PCM Solvation Calculations, *Inorg. Chem.*, 2005, **44**(11), 4024–4028.

29 I. Mayer, Bond order and valence indices: A personal account, *J. Comput. Chem.*, 2007, **28**(1), 204–221.